

Electromagnetic Absorption of Gaussian Beams by a Grounded Layered Structure

Constantinos A. VALAGIANNOPOULOS

Department of Radio Science and Engineering, School of Electrical Engineering,
Aalto University, Finland, PO Box 13000, FIN-00076 AALTO

konstantinos.valagiannopoulos@aalto.fi

Abstract. *A layered structure of magnetodielectric slabs, backed with a perfectly conducting plane, is illuminated by a Gaussian beam. The permittivities and permeabilities of each layer are selected so that the incident field penetrates smoothly into the subsequent layers and sustains gradually greater losses when reaching the internal ones. The performance of the device as an absorber is estimated through a newly defined indicator and it has been found that the absorbing capacity of the structure could be very high. This qualitative factor is robust and efficient when identifying which of the considered parameters are critical or insignificant as far as the performance of the layered configuration is concerned.*

Keywords

Electromagnetic absorber, Gaussian beam, linear superposition.

1. Introduction

With the expanding and parallel use of multiple electronic and electrical devices into a confined room or area, various forms of interference are encountered due to disturbing signals. To prevent such unwanted modifications, several types of devices have been designed and developed, the most common of which are the electromagnetic absorbers. An electrically thin absorber, suitable for electromagnetic laboratories, with wide incidence angles and functional for both polarizations has been presented [1] and an omnidirectional cylindrical absorber made of metamaterials has been also analyzed [2]. A simple device that traps the incident electromagnetic field into a ferromagnetic slab is investigated in [3] where similar nanocomposites are found to combine advantages of both dielectric and magnetic absorbers by possessing significantly better characteristics. Furthermore, absorbing layers are used in numerical simulation modeling where perfectly matched and insulating boundaries are used to reduce the simulation volume [4].

Gaussian beams are usually employed as excitations in theoretical analyses of electromagnetic problems since they are successfully imitating the actual feeding procedures. Unlike other excitation types, such as plane wave or point source illumination, the Gaussian beam is realistic and commonly utilized in “real-world” configurations (e.g. laser systems). In [5], some fundamental considerations concerning Gaussian beams have been rigorously stated. In addition, a general method solving the problem of an obliquely incident Gaussian beam on an anisotropic and axially inhomogeneous slab has been developed [6], while the case of the illumination of a penetrable sphere under the same excitation has been studied in [7]. Finally, a Gaussian beam summation representation for half plane diffraction of an incident two-dimensional Gaussian beam that hits arbitrarily close to the edge is presented in [8]; it has been proven the virtue of the Gaussian beam excitation to test and evaluate the response of the considered configuration from every angle of incidence.

In this work, we combine the two aforementioned topics (electromagnetic absorbers, Gaussian beams) to investigate a grounded layered structure, comprised of stacked homogeneous magnetodielectric slabs, in terms of its absorption capacity. This specific combination of the two topics has not yet been explicitly analyzed in the bibliography and it has a clear practical dimension due to the realistic excitation type adopted. Of course the mathematical approach is neither new nor original but it is applied on a particular case that can be used “as is” in numerous simulations. The Gaussian beam is expressed as an integral of plane waves and the solution of the plane wave scattering of the regarded configuration is obtained after imposing the necessary boundary conditions. The total solution under Gaussian beam excitation is found based on the principle of linear superposition. The constituent characteristics of the materials are selected in a way that secures a smooth coupling with the vacuum background combined with high thermal losses. A new performance indicator, based on the back reflected power before and after the installation of the layered structure, has been defined. This quality index is very useful in identifying the contribution of each parameter to the effectiveness of the device. The variations of this quantity with respect to the defined parameters are discussed and the presented results indicate very satisfying absorption of the incident field.

2. Problem Statement

Consider the two-dimensional (2D) structure depicted in Fig. 1. A Gaussian beam with its source at the origin of the utilized Cartesian coordinate system (x, y, z) , illuminates normally a layered structure. This structure occupies the rectangular volume $L < y < (L + W)$ and is comprised by U regions, each of which is assigned to a serial number $u = 1, \dots, U$, defined by the inequalities $L_{u-1} < y < L_u$. The materials that fill the corresponding regions possess relative dielectric permittivities denoted by ϵ_{ru} and magnetically anisotropic with relative magnetic permeability tensors denoted by μ_{ru} . The last (U -th) layer is connected to a grounded, perfectly conducting plane (PEC) at $y = L + W$. The upper semi-infinite $y < L$ area is labeled as 0-th region and is vacuum (characteristic parameters ϵ_0, μ_0) for which $\epsilon_{r0} = \mu_{r0} = 1$. Mind that the electric field produced by the excitation generator has a single \mathbf{z} component and propagates along the \mathbf{y} axis of our coordinate system. Due to the 2D nature of our configuration, this property for the incident electric field (\mathbf{z} -polarization) carries over every single of the $(U + 1)$ considered regions of the device. The adopted time dependence is of the form $\exp(+j2\pi ft)$ and is being suppressed throughout the present analysis.

The structure described above can be used as a component in electromagnetic designs in order to define the limits of the simulation area. In particular, the layered construction could be suitable for truncating the lattices in Finite Difference Time Domain (FDTD) applications [9] or clipping the meshing volume in Method of Moments (MoM) implementation [10] instead of utilizing common Perfectly Matched Layer (PML) techniques [11]. Furthermore, similar layered slabs could serve absorbing purposes in experimental prototypes and constructions. More specifically, one would employ planar multiple slabs as an alternative to pyramidal periodic blocks.

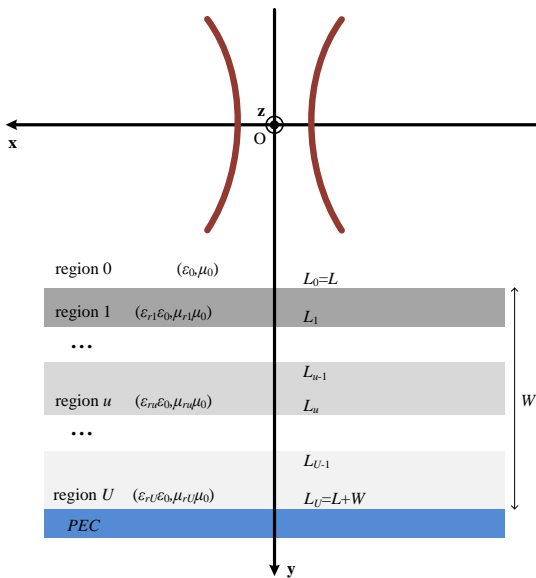


Fig. 1. The absorbing layered structure scatters the incident Gaussian beam.

Due to the aforementioned time dependence, the imaginary parts of the permittivities $\epsilon_{ru} = \Re[\epsilon_{ru}] + j\Im[\epsilon_{ru}]$ are negative which correspond to passive materials ($\Im[\epsilon_{ru}] < 0$), while the real parts are positive and larger than unity ($\Re[\epsilon_{ru}] > 1$). The same happens for the permeabilities μ_{ru} which are purely real ($\mu_{ru} > 1$). The described device is proposed to function as an efficient absorber; thus, the material transition from the one consecutive layer to the other should be fairly smooth. Therefore, we assume a linear increment of the characteristics of the material with respect to the related layer's serial number u , namely:

$$\epsilon_{ru} = 1 + (\epsilon_{rU} - 1) \frac{u}{U}, \quad (1)$$

$$\mu_{ru} = 1 + (\mu_{rU} - 1) \frac{u}{U}. \quad (2)$$

Furthermore, the thickness of each layer is taken equal to the others, for simplicity:

$$L_u = L + W \frac{u}{U}. \quad (3)$$

The aim of this work is to quantify the device's performance in trapping the normally incident Gaussian beam and identify which of the defined problem parameters affect more its capacity to work as absorber.

3. Incident Gaussian Beam

3.1 Approximate Expression

A Gaussian beam of \mathbf{z} -polarized electric field propagating into vacuum along the positive \mathbf{y} semi-axis possesses the following general form, valid for $y > 0$:

$$\mathbf{E}_{0,inc}(x, y) = \mathbf{z} \Pi(x, y) \exp(-jk_0 y) \quad (4)$$

where $k_0 = 2\pi f \sqrt{\epsilon_0 \mu_0}$ is the free space wavenumber and $\Pi(x, y)$ is the envelope of the beam. This envelope is reasonable to have an exponent proportional to $-x^2$ (to demonstrate the Gaussian nature), with a complex factor $\beta(y)$ dependent of y . If one considers an arbitrary amplitude function of y , $A(y)$, one concludes in the general formula: $\Pi(x, y) = A(y) \exp(-\beta(y)x^2)$, with $A(y), \beta(y) \in \mathbb{C}$ and $\Re[\beta(y)] \geq 0$. When substituting this expression for $\mathbf{E}_{0,inc}(x, y)$ to the vectorial Helmholtz equation into vacuum, the term proportional to $\frac{\partial^2 \Pi}{\partial y^2}$ can be ignored, since the rapid variation with respect to y is contained into the term $\exp(-jk_0 y)$. In this way, the following ordinary differential equations are obtained:

$$\beta'(y) + \frac{2}{jk_0} \beta^2(y) = 0 \Rightarrow \beta(y) = -\frac{k_0}{k_0 S + 2jy}, \quad (5)$$

$$A'(y) + \frac{\beta(y)}{jk_0} A(y) = 0 \Rightarrow A(y) = \frac{1}{\sqrt{k_0 S + 2jy}} \quad (6)$$

where $S \in \mathbb{C}$ is an arbitrary complex coefficient measured in square meters (m^2). Needless to say that the prime \prime corresponds to the first derivative of a function with respect to its

sole argument. Let us take $S = -\frac{2\chi}{k_0}$, where $\chi > 0$ is a length quantity. After careful separation of the real parts from the imaginary ones, the envelope function is found equal to:

$$\begin{aligned} \Pi(x, y) = & \sqrt[4]{\frac{4\chi}{R(\chi, y)}} \exp\left[\frac{j}{2} \arctan\left(\frac{y}{\chi}\right)\right] \cdot \\ & \exp\left[-x^2 \frac{k_0}{R(\chi, y)}\right] \exp\left[-jx^2 \frac{k_0}{R(y, \chi)}\right] \end{aligned} \quad (7)$$

where $R(y, \chi) = 2y \left[1 + \left(\frac{y}{\chi}\right)^2\right]$ a function with length dimension. We call the parameter χ ‘‘concentration length,’’ which expresses how concentrated is the power in the vicinity of the source ($y = 0$). In other words, a larger concentration length, indicates a smoother decaying behavior of the envelope as the observation points get distant from the \mathbf{x} axis when $y = 0$. This is not a strict definition for parameter χ ; it simply demonstrates a relation between χ and the envelope shape.

3.2 Fourier Expansion

Let us try a general approach in the first place. Assume a vectorial signal of the form $\mathbf{v}(x, y) = \mathbf{z} v(x, y)$ which follows the Helmholtz equation. If we take the projection of the \mathbf{z} component along the plane $y = 0$, a scalar signal which is an exclusive function of x has been obtained: $v(x, 0)$. By employing a very old tool such as the one-dimensional Fourier transform, the following dual set of equations is produced:

$$v(x, 0) = \frac{1}{2\pi} \int_{-\infty}^{+\infty} V(\alpha) \exp(j\alpha x) d\alpha, \quad (8)$$

$$V(\alpha) = \int_{-\infty}^{+\infty} v(x, 0) \exp(-j\alpha x) dx \quad (9)$$

where α is a real parameter corresponding to an incidence angle. In this way, a complex signal $v(x, 0)$ has been expressed as an integral of the exponential factors $\exp(j\alpha x)$. But if a signal $\mathbf{w}(x, y) = \mathbf{z} \exp(j\alpha x) w_y(y)$ satisfies the Helmholtz equation, then its y -dependence is readily found as: $w_y(y) = \exp(\pm y \sqrt{\alpha^2 - k_0^2})$. Therefore, by taking into account the integral (with direct use of MATHEMATICA, [12]):

$$\int_{-\infty}^{+\infty} \Pi(x, 0) \exp(-j\alpha x) dx = \sqrt[4]{2} \sqrt{\frac{2\pi\chi}{k_0}} \exp\left(-\frac{\chi\alpha^2}{2k_0}\right), \quad (10)$$

and given the fact that the incident field $\mathbf{v} = \mathbf{E}_{0,inc}$ obeys the vectorial Helmholtz equation, it is written in integral form:

$$\begin{aligned} \mathbf{E}_{0,inc}(x, y) = & \mathbf{z} \sqrt[4]{2} \sqrt{\frac{\chi}{2\pi k_0}} \cdot \\ & \int_{-\infty}^{+\infty} \exp\left(-\frac{\chi\alpha^2}{2k_0}\right) \exp\left(j\alpha x - y \sqrt{\alpha^2 - k_0^2}\right) d\alpha. \end{aligned} \quad (11)$$

The square roots are evaluated with a positive sign $\Re[\sqrt{\star}] > 0$, and in case it equals zero, with a positive imaginary sign

$\Im[\sqrt{\star}] > 0$. The aforementioned formula (11) is suitable for points $y > 0$, otherwise the sign of the related exponential in w_y should be reversed (the same should be done for the sign of the exponential component $\exp(-jk_0 y)$ in (4)). It should be stressed that (11) is not equivalent to the expression $\mathbf{E}_{0,inc}(x, y) = \mathbf{z} \Pi(x, y) \exp(-jk_0 y)$ since the latter one only approximately obeys the Helmholtz equation (the term proportional to $\frac{\partial^2 \Pi}{\partial y^2}$ has been ignored as insignificant). Assume now that one excites an arbitrary 2D configuration at $y > 0$ with a \mathbf{z} -polarized planar wave into vacuum $\mathbf{e}_{inc}(x, y, \alpha) = \mathbf{z} \exp(j\alpha x - y \sqrt{\alpha^2 - k_0^2})$, which is propagating for $|\alpha| < k_0$ and evanescent for $|\alpha| > k_0$. If one computes the scattered field $\mathbf{e}_{scat}(x, y, \alpha)$ under plane wave excitation into each of the considered regions, the corresponding response field for a Gaussian beam illumination is computed by acting with the following operator:

$$\mathcal{J}\{\star\} = \sqrt[4]{2} \sqrt{\frac{\chi}{2\pi k_0}} \int_{-\infty}^{+\infty} \exp\left(-\frac{\chi\alpha^2}{2k_0}\right) \star d\alpha, \quad (12)$$

on the scattering field vector $\mathbf{e}_{scat}(x, y, \alpha)$. Such a general conclusion is directly based on the fundamental principle of superposition and the linearity of the Maxwell’s equations. The factor $\exp\left(-\frac{\chi\alpha^2}{2k_0}\right)$ guarantees the convergence of the integral for $|\alpha| \rightarrow +\infty$.

4. Absorbing Layered Structure

4.1 Plane Wave Solution

The mathematical methods utilized in the following, have been thoroughly developed and described in part or as a whole in numerous works such as [17]-[20]. We assume that the structure is excited by the plane wave:

$$\mathbf{e}_{0,inc}(x, y, \alpha) = \mathbf{z} \exp\left(j\alpha x - y \sqrt{\alpha^2 - k_0^2}\right) \quad (13)$$

where $\alpha \in \mathbb{R}$ can be any real number. The case $\alpha = 0$ corresponds to a normal incidence to the layered structure. The reflected electric field of region 0, due to phase matching of $\exp(j\alpha x)$ along the horizontal plane $y = L$, is given by:

$$\mathbf{e}_{0,ref}(x, y, \alpha) = \mathbf{z} \rho(\alpha) \exp\left[j\alpha x + (y - L) \sqrt{\alpha^2 - k_0^2}\right] \quad (14)$$

where $\rho(\alpha)$ is the reflection coefficient complex function of the entire structure. The electric field into the u -th region is given by the formula:

$$\begin{aligned} \mathbf{e}_u(x, y, \alpha) = & \mathbf{z} \{A_u(\alpha) \exp[-\gamma_u(\alpha)(y - L_u)] \\ & + B_u(\alpha) \exp[\gamma_u(\alpha)(y - L_u)]\} \exp(j\alpha x). \end{aligned} \quad (15)$$

The auxiliary radiation quantity γ_u is defined as:

$$\gamma_u(\alpha) = \sqrt{\alpha^2 - k_0^2 \epsilon_{ru} \mu_{ru}} \quad (16)$$

where $\epsilon_{ru} = \Re[\epsilon_{ru}] + j\Im[\epsilon_{ru}]$ with $\Re[\epsilon_{ru}] > 1$ and $\Im[\epsilon_{ru}] < 0$.

If one imposes the related boundary conditions for continuous tangential electric and magnetic components along the representative separating plane $z = L_u, u \neq 0, U$, one obtains the matrix relation:

$$\begin{bmatrix} A_u(\alpha) \\ B_u(\alpha) \end{bmatrix} = \mathbf{T}_u(\alpha) \cdot \begin{bmatrix} A_{u+1}(\alpha) \\ B_{u+1}(\alpha) \end{bmatrix} \Rightarrow \begin{bmatrix} A_1(\alpha) \\ B_1(\alpha) \end{bmatrix} = \mathbf{T}_1(\alpha) \cdots \mathbf{T}_{U-1}(\alpha) \cdot \begin{bmatrix} A_U(\alpha) \\ B_U(\alpha) \end{bmatrix} \quad (17)$$

where \mathbf{T}_u is a 2×2 transfer matrix whose elements are given by:

$$[\mathbf{T}_u(\alpha)]_{11} = \frac{\gamma_{u+1}(\alpha)\mu_{ru} + \gamma_u(\alpha)\mu_{r(u+1)}}{2\gamma_u(\alpha)\mu_{r(u+1)}} e^{\gamma_{u+1}(\alpha)\Delta L_u}, \quad (18)$$

$$[\mathbf{T}_u(\alpha)]_{12} = -\frac{\gamma_{u+1}(\alpha)\mu_{ru} - \gamma_u(\alpha)\mu_{r(u+1)}}{2\gamma_u(\alpha)\mu_{r(u+1)}} e^{-\gamma_{u+1}(\alpha)\Delta L_u}, \quad (19)$$

$$[\mathbf{T}_u(\alpha)]_{21} = -\frac{\gamma_{u+1}(\alpha)\mu_{ru} - \gamma_u(\alpha)\mu_{r(u+1)}}{2\gamma_u(\alpha)\mu_{r(u+1)}} e^{\gamma_{u+1}(\alpha)\Delta L_u}, \quad (20)$$

$$[\mathbf{T}_u(\alpha)]_{22} = \frac{\gamma_{u+1}(\alpha)\mu_{ru} + \gamma_u(\alpha)\mu_{r(u+1)}}{2\gamma_u(\alpha)\mu_{r(u+1)}} e^{-\gamma_{u+1}(\alpha)\Delta L_u} \quad (21)$$

where $\Delta L_u = L_{u+1} - L_u$. The same techniques are used for analyzing similar structures [13]-[16]. The boundary conditions along the upper and the lower surfaces $y = L, (L + W)$ are written as follows:

$$\begin{bmatrix} A_0(\alpha) \\ B_0(\alpha) \end{bmatrix} = \mathbf{g}_0(\alpha)\rho(\alpha) + \mathbf{q}_0(\alpha), \quad (22)$$

$$\begin{bmatrix} A_U(\alpha) \\ B_U(\alpha) \end{bmatrix} = \mathbf{g}_U A_U(\alpha) \quad (23)$$

where the participating vectors are defined below:

$$\mathbf{g}_0(\alpha) = \begin{bmatrix} \frac{\gamma_1(\alpha) - \gamma_0(\alpha)\mu_{r1}}{2\gamma_1(\alpha)} e^{-\gamma_1(\alpha)(L_1 - L)} \\ \frac{\gamma_1(\alpha) + \gamma_0(\alpha)\mu_{r1}}{2\gamma_1(\alpha)} e^{\gamma_1(\alpha)(L_1 - L)} \end{bmatrix}, \quad (24)$$

$$\mathbf{q}_0(\alpha) = \begin{bmatrix} \frac{\gamma_1(\alpha) + \gamma_0(\alpha)\mu_{r1}}{2\gamma_1(\alpha)} e^{-\gamma_1(\alpha)(L_1 - L) - \gamma_0(\alpha)L} \\ \frac{\gamma_1(\alpha) - \gamma_0(\alpha)\mu_{r1}}{2\gamma_1(\alpha)} e^{\gamma_1(\alpha)(L_1 - L) - \gamma_0(\alpha)L} \end{bmatrix}, \quad (25)$$

$$\mathbf{g}_U = \begin{bmatrix} 1 \\ -1 \end{bmatrix}. \quad (26)$$

By combining the relations (17), (22) and (23), the following 2×2 linear system is obtained. The unknown reflection and transmission coefficients are readily found:

$$\begin{bmatrix} -\mathbf{g}_0(\alpha) & \mathbf{M}(\alpha) \cdot \mathbf{g}_U \end{bmatrix} \cdot \begin{bmatrix} \rho(\alpha) \\ A_U(\alpha) \end{bmatrix} = \mathbf{q}_0(\alpha) \Rightarrow \begin{bmatrix} \rho(\alpha) \\ A_U(\alpha) \end{bmatrix} = \begin{bmatrix} -\mathbf{g}_0(\alpha) & \mathbf{M}(\alpha) \cdot \mathbf{g}_U \end{bmatrix}^{-1} \cdot \mathbf{q}_0(\alpha) \quad (27)$$

where $\mathbf{M}(\alpha) = \mathbf{T}_1(\alpha) \cdots \mathbf{T}_{U-1}(\alpha)$. In this way, the scattering problem under plane wave excitation has been solved.

4.2 Output Quantity

The complex function $\rho(\alpha)$ is describing the behavior of the structure for different types of plane-wave excitation. In fact, it is a kind of “transfer function” which tests and evaluates the reaction of the device for excitations along the entire spatial spectrum $\alpha \in \mathbb{R}$. Once the expression of this function is determined from (27), one can compute the total reflected field of the Gaussian scattering problem with use of the operator defined in (12):

$$\mathbf{E}_{0,ref}(x, y) = \mathcal{J} \{ \mathbf{e}_{0,ref}(x, y, \alpha) \} = \sqrt[4]{2} \sqrt{\frac{\chi}{2\pi k_0}} \int_{-\infty}^{+\infty} \exp\left(-\frac{\chi\alpha^2}{2k_0}\right) \mathbf{e}_{0,ref}(x, y, \alpha) d\alpha. \quad (28)$$

The parameter χ (concentration length) is the only degree of freedom characterizing and describing the incident propagation wave constituting the Gaussian beam. In this sense, the reflecting power of the overall problem along a distance $2h$ of \mathbf{x} axis on the separating plane $y = L$ is defined as follows:

$$P_{ref}(h) = \int_{-h}^h |\mathbf{z} \cdot \mathbf{E}_{0,ref}(x, L)|^2 dx. \quad (29)$$

We call the distance h the “integration length” which depends positively the calculated portion of the reflected power.

To estimate the performance of the proposed device we should introduce a ratio called “absorption factor” (\mathcal{AF}):

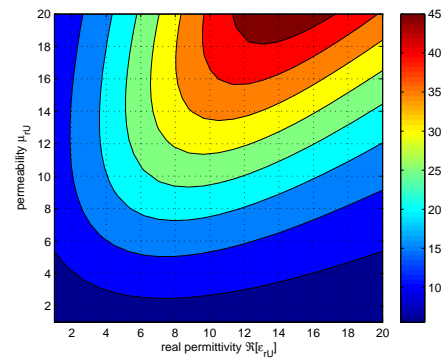
$$\mathcal{AF}(h) = \frac{\tilde{P}_{ref}(h)}{P_{ref}(h)} \quad (30)$$

where $\tilde{P}_{ref}(h)$ is the reflected power along the integration length h , in the absence of the layered absorber, namely when $\epsilon_{ru} = \mu_{ru} = 1$ for $u = 1, \dots, U$. The reflection coefficient function in this case, equals $\tilde{\rho}(\alpha) = \exp[-(L + 2W)\gamma_0(\alpha)]$. Apparently, the higher is the absorption factor evaluated, the more efficient is the operation of the described device as absorber. For a structure with $\mathcal{AF} \gg 1$, the reflected power would be much less compared to the case of an absent layered slab where total reflection is occurred. This factor would be the sole output quantity whose variation is represented in the graphs of the next Section 5.

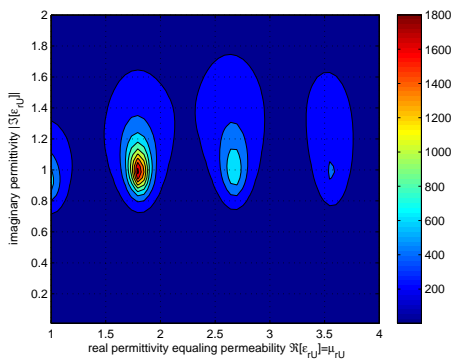
5. Numerical Results

5.1 Parameter Ranges

Let us define the ranges of the input parameters that are used in the defined problem. First of all, the operational frequency f is chosen to belong into the radio band, namely around the central frequency $f_0 = 12$ GHz (corresponding to the wavelength $\lambda_0 = c/f_0 = 2.5$ cm where $c = 3 \cdot 10^8$ m/sec is the speed of electromagnetic waves into vacuum) which serves also normalization purposes. The extracted conclusions of course can be easily carried over to other bands



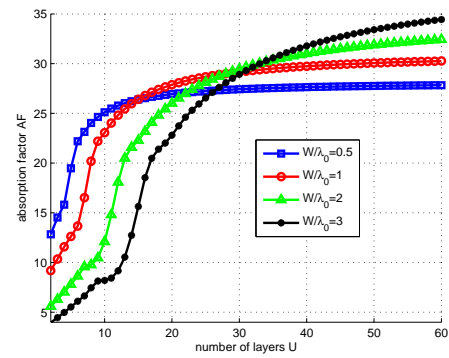
(a)



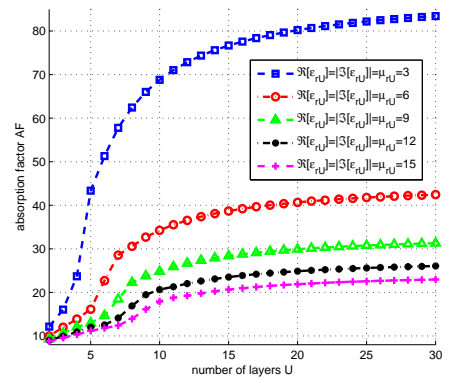
(b)

Fig. 2. Contour plots of the absorption factor \mathcal{AF} with respect to: (a) the real relative permittivity $\Re[\epsilon_{rU}]$ and the relative permeability μ_{rU} ($|\Im[\epsilon_{rU}]| = 10$) and (b) the real relative permittivity $\Re[\epsilon_{rU}]$, when it is equal to the relative permeability μ_{rU} , and the absolute imaginary permittivity $|\Im[\epsilon_{rU}]|$. Plot parameters: $f_0 = 12$ GHz, $\lambda_0 = c/f_0 = 2.5$ cm, $f = f_0$, $U = 15$, $W = \lambda_0$, $L = 0.5\lambda_0$, $\chi = 0.2\lambda_0$, $h = \lambda_0$.

since the electrical sizes are that which count. The real, the (absolute) imaginary part of the permittivity of the last (U -th) layer and also the relative permeability in the same region, are selected to be less than an order of 20, namely: $1 < \Re[\epsilon_{rU}]$, $\mu_{rU} < 20$ and $0 < |\Im[\epsilon_{rU}]| < 20$. As stated in Section II, the intrinsic parameters of the last layer, determine the characteristics in every other equi-sized layer through the relations: $\epsilon_{ru} = 1 + (\epsilon_{rU} - 1) \frac{u}{U}$ and $\mu_{ru} = 1 + (\mu_{rU} - 1) \frac{u}{U}$ for $u = 1, \dots, U$. The number of layers U can vary within the interval: $2 < U < 20$ and the length h , along which the reflected power is evaluated, is usually chosen with relatively large electrical value $0.5 < h/\lambda_0 < 3$. The thickness of the layered structure is also large ($0.5 < W/\lambda_0 < 3$), while the electrical distance of the Gaussian beam from the first layer possesses electrically moderate magnitudes ($0.1 < L/\lambda_0 < 1$). As far as the normalized concentration length is concerned, it covers the range: $0.01 < \chi/\lambda_0 < 0.5$.



(a)



(b)

Fig. 3. The absorption factor \mathcal{AF} as function of the number of layers U for several: (a) normalized thicknesses of the slab W/λ_0 ($\Re[\epsilon_{rU}] = -\Im[\epsilon_{rU}] = \mu_{rU} = 10$) and (b) real relative permittivities $\Re[\epsilon_{rU}]$ being equal to the absolute imaginary permittivities $|\Im[\epsilon_{rU}]|$ and the relative permeabilities μ_{rU} ($W = \lambda_0$). Plot parameters: $f_0 = 12$ GHz, $\lambda_0 = c/f_0 = 2.5$ cm, $f = f_0$, $L = 0.5\lambda_0$, $\chi = 0.2\lambda_0$, $h = \lambda_0$.

5.2 Graphs Discussion

In Fig. 2(a), we show the variation of the absorption factor \mathcal{AF} , in contour plot, with respect to the real part of the relative permittivity $\Re[\epsilon_{rU}]$ and the relative permeability μ_{rU} . The imaginary part is kept constant and equal to: $\Im[\epsilon_{rU}] = -10$. With a fixed μ_{rU} , the evaluated quantity is increasing for smaller $\Re[\epsilon_{rU}]$ and decreasing for larger ones by achieving a local maximum close to $\Re[\epsilon_{rU}] \cong \mu_{rU}$. When both variables get increased with the same pace, the performance of the corresponding absorber is increased. In Fig. 2(b), the absorption factor is presented again in a contour map with its horizontal axis corresponding to $\Re[\epsilon_{rU}]$, which is now taken equal to μ_{rU} , and a vertical axis counting the absolute value of the imaginary part of the relative permittivity $|\Im[\epsilon_{rU}]|$. One can clearly notice that the magnitudes \mathcal{AF} are way higher than in Fig. 2(a), due to the condition

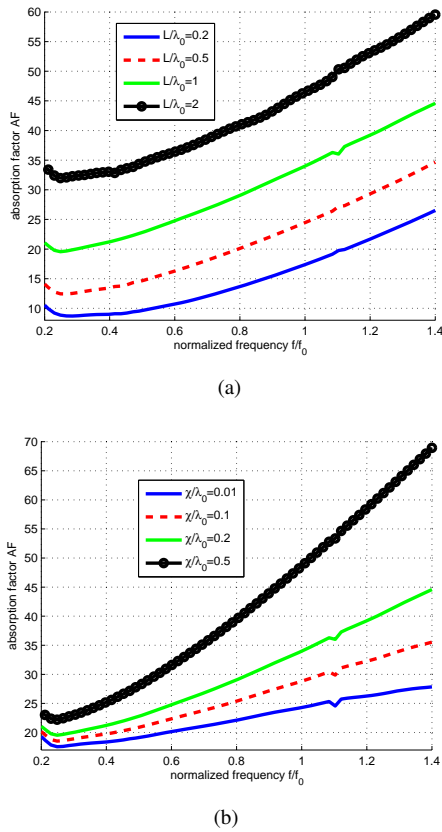


Fig. 4. The absorption factor \mathcal{AF} as function of the normalized frequency f/f_0 for several: (a) electrical distances L/λ_0 ($\chi = 0.2\lambda_0$) and (b) normalized concentration lengths χ/λ_0 ($L = \lambda_0$). Plot parameters: $f_0 = 12$ GHz, $\lambda_0 = c/f_0 = 2.5$ cm, $W = \lambda_0$, $h = 2\lambda_0$, $\Re[\epsilon_{rU}] = -\Im[\epsilon_{rU}] = \mu_{rU} = 10$.

$\Re[\epsilon_{rU}] = \mu_{rU}$ which indicates a surface matched to the vacuum background. Note also that in the vicinity of the line $\Im[\epsilon_{rU}] = -1$, several local maxima are observed, each of which corresponds to a perfect absorber.

In Fig. 3(a), our sole output quantity \mathcal{AF} is presented as function of the number U of layers for several thicknesses of the structure W/λ_0 . Naturally, the absorption factor gets gradually improved for increasing U as the material discontinuities get milder and the reflections less significant. Note also that after a certain number U (different for each case), the curve tends to a final value \mathcal{AF} , which corresponds to the continuously inhomogeneous slab. In case the absorber is thicker (larger W/λ_0), the behavior is stabilized at higher U due to the slower discretization convergence for larger electrical sizes; additionally, the performance is better since the transition is carried out in a smoother way. It is also noteworthy that when $U < 15$, thinner substrates absorb more effectively the incident Gaussian beam; such a feature is attributed to the decreased size of the discontinuous adjacent layers. In other words, the maximum electrical size of the layer for which a smooth transition is achieved, is reached for smaller U , when thicknesses W/λ_0 are moderate. In Fig. 3(b), the variation of the absorp-

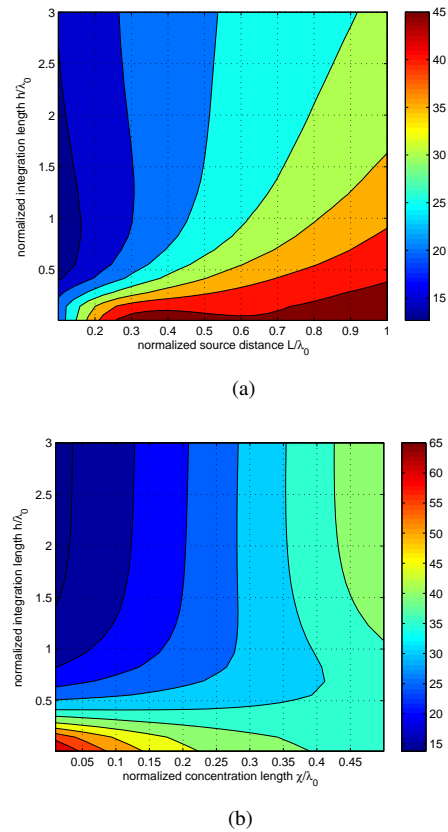


Fig. 5. Contour plots of the absorption factor \mathcal{AF} with respect to: (a) the source electrical distance L/λ_0 and the normalized integration length h/λ_0 ($\chi = 0.2\lambda_0$) and (b) the normalized concentration length χ/λ_0 and the normalized integration length h/λ_0 ($L = 0.5\lambda_0$). Plot parameters: $f_0 = 12$ GHz, $\lambda_0 = c/f_0 = 2.5$ cm, $f = f_0$, $U = 15$, $W = \lambda_0$, $\Re[\epsilon_{rU}] = -\Im[\epsilon_{rU}] = \mu_{rU} = 10$.

tion factor is depicted with respect to U for various materials of the bottom (U -th) layer under the simplifying condition: $\Re[\epsilon_{rU}] = |\Im[\epsilon_{rU}]| = \mu_{rU}$. Again, the same behavior for increasing U is observed as in Fig. 3(a). It is though remarkable that higher losses (larger $|\Im[\epsilon_{rU}]|$) do not lead necessarily to more efficient absorbers since the imperfect conductors for $|\Im[\epsilon_{rU}]| \rightarrow +\infty$ behave as perfect ones inflicting total reflection (and zero absorption). In particular, the higher \mathcal{AF} is recorded for $\Im[\epsilon_{rU}] = -3$ and the situation is even better for $\Im[\epsilon_{rU}] = -1$ as indicated in Fig. 2(b). Needless to say, that no absorption is achieved with a grounded lossless slab ($\Im[\epsilon_{rU}] = 0$). In other words, one can retain an equilibrium avoiding not only highly lossy materials with their poor coupling with the vacuum background but also slightly lossy materials with their weak absorption capacity as well.

In Fig. 4(a), the absorption factor is represented as function of the normalized operational frequency f/f_0 for different source electrical distances L/λ_0 . One can readily identify that the proposed device is more functional when the source of the beam is located far from the absorbing slab. This is an anticipated result since the incident field resembles more a plane wave when L/λ_0 is large and thus is negligibly reflected from the matched surface. It should be

stressed that the transmission-line theory and the notion of impedance matching [21] assumes normally incident waves such those constituting the excitation field for large L/λ_0 . Consequently, for $L/\lambda_0 \rightarrow +\infty$, the primary fields penetrate almost totally into the structure and attenuate due to high losses. In all cases, the performance is improved for larger frequencies because the equiphase surfaces of the incident wave get more rapidly converted into planes. In Fig. 4(b), the factor \mathcal{AF} is shown with respect to normalized operational frequency f/f_0 for different normalized concentration lengths χ/λ_0 . Again, the result is poor for smaller χ/λ_0 since the wave components corresponding to oblique incidence ($\alpha \neq 0$) become more significant and thus more substantial reflections are appeared. The distance gap between the upward sloping curves is opening for increasing frequency contrary to Fig. 4(b), where the differences are kept rather constant.

In Fig. 5(a), the variation of \mathcal{AF} is presented in contour plot as function of the electrical source distance L/λ_0 and the normalized integration length h/λ_0 . The recorded quantity is stabilized for larger h/λ_0 which means that the integral (29) gives the total reflected power ($h \rightarrow +\infty$). This convergence is achieved more easily when L/λ_0 is small; this is natural, since the distribution of the incident field along the surface $y = L$ gets more concentrated when the source is posed closer to the slab. In Fig. 5(b), we show the magnitude of the absorption factor on a map with the normalized concentration length of the Gaussian beam at its horizontal axis and the normalized integration length h/λ_0 at its vertical. Note that for most integration lengths $h/\lambda_0 > 0.5$, the dependence of \mathcal{AF} on h/λ_0 gets weaker regardless of the corresponding concentration length. This feature is demonstrated by the vertical iso-contour lines at the upper half of the considered diagram.

In Fig. 6(a), this performance indicator \mathcal{AF} is shown as function of the real permittivity $\Re[\epsilon_{rU}]$ in case a uniform superstrate is used ($U = 1$) for several electrical thicknesses W/λ_0 . Similarly, in Fig. 6(b) the independent variable is the uniform magnetic permeability μ_{rU} of the single layer. From both the graphs, it is clear that poor absorption performance is achieved when only one lossy superstrate is employed. In particular, for the uniform case ($U = 1$), we obtain $\mathcal{AF} < 20$, while in all the other graphs (where $U > 2$) the optimal absorption factor is several times larger. Accordingly, the use of multilayered structures is necessary to accomplish satisfying results.

6. Conclusion

A grounded stack of dielectric slabs is excited by a normally incident Gaussian beam. The plane wave solution of the problem is integrated with respect to the angle of incidence to obtain the overall solution and compute the reflected power from the layered structure. It has been found that the reflections are much diminished compared to the case of absent layers.

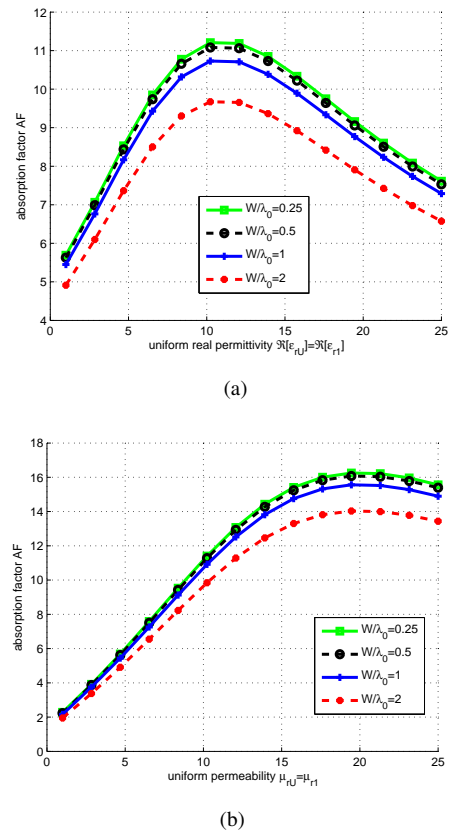


Fig. 6. The absorption factor \mathcal{AF} as function of the: (a) uniform real permittivity $\Re[\epsilon_{rU}] = \Re[\epsilon_{r1}]$ ($\mu_{rU} = \mu_{r1} = 10$, $|\Im[\epsilon_{rU}]| = |\Im[\epsilon_{r1}]| = 10$) and (b) uniform permeability $\mu_{rU} = \mu_{r1}$ for various electrical thicknesses W/λ_0 ($\Re[\epsilon_{rU}] = \Re[\epsilon_{r1}] = 10$, $|\Im[\epsilon_{rU}]| = |\Im[\epsilon_{r1}]| = 10$). Plot parameters: $f_0 = 12$ GHz, $\lambda_0 = c/f_0 = 2.5$ cm, $h = 2\lambda_0$, $\chi = 0.2\lambda_0$.

An interesting expansion of the present work would be to use chiral, anisotropic or bianisotropic materials to construct the layered absorber. The extra degrees of freedom could be exploited in order to achieve higher performance by using more directly found substances or more easily realizable artificial materials. In addition, the shape of the structure could be modified in order to simulate different configurations befitted to three-dimensional excitations. Comparison between Cartesian, cylindrical, spherical and other versions of the same layered structures can be made in order to obtain optimized results. In this way, similar conclusions for more realistic designs can be drawn.

References

- [1] LUUKKONEN, O., COSTA, F., SIMOVSKI, C. R., MONORCHIO, A., TRETYAKOV, S. A. A thin electromagnetic absorber for wide incidence angles and both polarizations. *IEEE Transactions on Antennas and Propagation*, 2009, vol. 57, no. 10, p. 3119 - 3125.
- [2] CHENG, Q., CUI, T. J., JIANG, W. X., CAI, B. G. An omnidirectional electromagnetic absorber made of metamaterials. *New Journal of Physics*, 2010, vol. 12, 063006.

- [3] BREGAR, V. B. Advantages of ferromagnetic nanoparticle composites in microwave absorbers. *IEEE Transactions on Magnetics*, 2004, vol. 40, no. 3, p. 1679 - 1684.
- [4] ZIOLKOWSKI, R. W. The design of Maxwellian absorbers for numerical boundary conditions and for practical applications using engineered artificial materials. *IEEE Transactions on Antennas and Propagation*, 1997, vol. 45, no. 4, p. 656 - 671.
- [5] KRIEZIS, E. E., PANDELAKIS, P. K., PAPAGIANNAKIS, A. G. Diffraction of a Gaussian beam from a periodic planar screen. *Journal of the Optical Society of America A*, 1994, vol. 11, no. 2, p. 630 - 636.
- [6] LANDRY, G. D., MALDONADO, T. A. Gaussian beam transmission and reflection from a general anisotropic multilayer structure. *Applied Optics*, 1996, vol. 35, no. 30, p. 5870 - 5879.
- [7] KHALED, E. E. M., HILL, S. C., BARBER, P. W. Scattered and internal intensity of a sphere illuminated with a Gaussian beam. *IEEE Transactions on Antennas and Propagation*, 1993, vol. 41, no. 3, p. 295 - 303.
- [8] KATSAV, M., HEYMAN, E. Gaussian beam summation representation of a two-dimensional Gaussian beam diffraction by a half plane. *IEEE Transactions on Antennas and Propagation*, 2007, vol. 55, no. 8, p. 2247 - 2257.
- [9] PAUK, L., SKVOR, Z. FDTD stability: critical time increment, *Radioengineering*, 2003, vol. 12, no. 2, p. 16 - 22.
- [10] VALAGIANNOPOULOS, C. A. A novel methodology for estimating the permittivity of a specimen rod at low radio frequencies. *Journal of Electromagnetic Waves and Applications*, 2010, vol. 24, no. 5-6, p. 631 - 640.
- [11] YANG, J., HUANG, M. YANG, C. SHI, J. Arbitrary shape electromagnetic transparent device based on Laplaces equation. *Radioengineering*, 2011, vol. 20, no. 1, p. 307 - 311.
- [12] *On-line Integrator from Wolfram Research*. [Online] Available at: <http://integrals.wolfram.com/index.jsp>.
- [13] VALAGIANNOPOULOS, C. A. Effect of cylindrical scatterer with arbitrary curvature on the features of a metamaterial slab antenna. *Progress in Electromagnetic Research*, 2007, vol. 71, p. 59 - 83.
- [14] VALAGIANNOPOULOS, C.A., TSITSAS, N. L. Linearization of the T-matrix solution for quasi-homogeneous scatterers. *Journal of the Optical Society of America A*, 2009, vol. 26, no. 4, p. 870 - 881.
- [15] VALAGIANNOPOULOS, C. A. Electromagnetic scattering of the field of a metamaterial slab antenna by an arbitrarily positioned cluster of metallic cylinders. *Progress in Electromagnetic Research*, 2011, vol. 114, p. 51 - 66.
- [16] VALAGIANNOPOULOS, C. A. On adjusting the characteristics of a low-index slab antenna with a finite set of metallic pins. In *Proceedings of the 5th European Conference on Antennas and Propagation (EUCAP)*. Rome (Italy), 2011, p. 913 - 917.
- [17] VALAGIANNOPOULOS, C. A. Closed-form solution to the scattering of a skew strip field by metallic pin in a slab. *Progress in Electromagnetic Research*, 2008, vol. 79, p. 1 - 21.
- [18] VALAGIANNOPOULOS, C. A., UZUNOGLU, N. K. Rigorous analysis of a metallic circular post in a rectangular waveguide with step discontinuity of sidewalls. *IEEE Transactions on Microwave Theory and Techniques*, 2007, vol. 55, no. 8, p. 1673 - 1684.
- [19] VALAGIANNOPOULOS, C. A. A novel methodology for estimating the permittivity of a specimen rod at low radio frequencies. *Journal of Electromagnetic Waves and Applications*, 2010, vol. 24, no. 5-6, p. 631 - 640.
- [20] VALAGIANNOPOULOS, C. A., SIHVOLA, A. H. On modeling perfectly conducting sharp corners with magnetically inert dielectrics of extreme complex permittivities. *IEEE Transactions on Antennas and Propagation*, 2012, vol. 60, no. 10, p. 4777 - 4784.
- [21] VALAGIANNOPOULOS, C. A., ALITALO, P. Electromagnetic cloaking of cylindrical objects by multilayer or uniform dielectric claddings. *Physical Review B*, 2012, vol. 85, 115402.

About Author ...

Constantinos VALAGIANNOPOULOS was born in Athens, Greece in 1982. He received the Dipl. Eng. degree in Electrical Engineering from National Technical University of Athens (NTUA) in 2004, and the Ph.D. degree for studies on Electromagnetic Theory in 2009. He has also graduated from Athens University of Economics and Business (AUEB) with specialization in Financial Engineering. From 2010, he works as a postdoctoral researcher in the Department of Radio Science and Engineering of the Aalto University, Finland. Dr. Valagiannopoulos's research interests include Electromagnetics, Applied Mathematics and Physics. He has authored or coauthored over 35 works in international refereed scientific journals and presented numerous reports in international refereed scientific conferences. Dr. Valagiannopoulos was the recipient of the International Chorafas Prize for the Best Doctoral Thesis in 2008 and the Academy of Finland Postdoctoral Grant for 2012-2015.